IEEE Access
Multidisciplinary | Rapid Review | Open Access Journal

Received 8 June 2022, accepted 24 July 2022, date of publication 5 August 2022, date of current version 10 August 2022.

Digital Object Identifier 10.1109/ACCESS.2022.3196672

RESEARCH ARTICLE

Volume Signaling and Neural-Indexing by Nitric Oxide in Artificial Neural Networks

PABLO FERNÁNDEZ-LÓPEZ[1], PATRICIO GARCÍA-BÁEZ[2], YLERMI CABRERA-LEÓN[1], JUAN L. NAVARRO-MESA[3], (Member, IEEE), AND CARMEN PAZ SUÁREZ-ARAUJO[1]

[1]Institute for Cybernetic Science and Technologies (IUCTC), University of Las Palmas de Gran Canaria, 35017 Las Palmas, Spain
[2]Department of Computer Engineering and Systems, University of La Laguna, 38206 San Cristóbal de La Laguna, Spain
[3]Institute for Technological Development and Innovation in Communication (IDeTIC), University of Las Palmas de Gran Canaria, 35017 Las Palmas, Spain

Corresponding author: Carmen Paz Suárez-Araujo (carmenpaz.suarez@ulpgc.es)

This work was supported in part by the "Consejería de Vicepresidencia Primera y de Obras Públicas, Infraestructuras, Transporte y Movilidad del Cabildo de Gran Canaria," under Grant 23/2021.

ABSTRACT We present a computational study whose objective is to show the capacity of the Nitric Oxide (NO) diffusion for information recovery and indexing related to the classical neural architecture Sparse Distributed Memory (SDM). The study is carried out by introducing NO diffusion dynamics by means of a Multi-compartment based NO Diffusion Model in the storage process of the SDM. We develop a new SDM model, which we term Sparse Distributed Memory by Nitric Oxide diffusion (SDM-NO). Both of these architectures were computationally analysed. We have shown that the information indexing guided by the Nitric Oxide dynamics has a similar or slightly better behaviour to the randomly guided indexing by the SDM. Two kinds of patterns were used in the study: a) binary string patterns with eight bits and b) handwritten characters. The indexing guided by the Nitric Oxide dynamics shows a similar or a little bit better behaviour to the guided indexing one performed randomly by the SDM. Nevertheless, we have also shown that both of the architectures do not perform well in these memory processes.

INDEX TERMS Artificial neural network, nitric oxide, nitric oxide dynamic, neural-indexing, sparse distributed memory.

I. INTRODUCTION

Nitric Oxide (NO) is one of the seminal events in physiology, physio-pathological and vascular research. It was independently discovered by different research groups [1]–[4], when at the end of the 1980′s its role as a neurotransmitter on the nervous system was studied [5]–[7].

NO, together with Carbon Monoxide (CO) and Hydrogen Sulfide (H_2S) (gases that also show functions of signaling) belong to the group of most toxic substances and are synthesized by numerous organisms that carry out the transmission of information function [8]. NO participates in essential neural signaling functions, not only in the Peripheral Nervous System (PNS), but also in the Central Nervous System (CNS). In the PNS it acts as a control element in cardiovascular, respiratory, and digestive systems. NO acts as a retrograde neurotransmitter in the CNS [9], [10]. Thus, the hippocampus and the cortex are involved in Long Term Potentiation (LTP), produced in the postsynaptic environment and acting in the presynaptic environment [11]–[15]. Long term depression (LTD) seems to be involved in the cerebellum and striate nucleus, where signals are carried out from the presynaptic to the postsynaptic environment. In addition, NO is one of the known retrograde messengers of the Biological Neural Network (BNN) with implications for learning and memory. It participates in different types of synaptic plasticity, in functions of synchronization of neural activity and in the blood flow from the brain. NO contributes in functions of stabilization of the synaptic efficiency and ease of the release of the neurotransmitters, as well in the directionality of dendritic tree growth [10].

Physical-chemical phenomena different to those produced in non-neural tissues are not observed in the brain [16], however it has a greater ability to generate electrical phenomena,

The associate editor coordinating the review of this manuscript and approving it for publication was Manuel Rosa-Zurera.

a special characteristic and one which seems to support its own computational capacity [17]. This ability is similar to the behaviour of any living being resides in the brain. Such behavior is recognized as a weighted phenomenon between genes and environment [15], where learning and memory act as specific mechanisms that modulate such behavior through environmental events.

Learning is the capacity for a system to absorb knowledge from the environment without external programming. The process of learning is how living beings modify their knowledge of the outside world (changes in the nervous system that result from the experience and originate lasting changes in the behavior of living beings). Memory is understood as the retention or storage of said knowledge. Understanding memory means to understand how different concepts are stored and recovered which are involved in the creation of our thoughts. Connected to all of this is the overlapping of these concepts, and closely related to this is how they are linked to each other, or how some of them are activated when others are evoked. In this context, the concept of the BNN information indexing is needed.

These mechanisms are involved in memory and in learning and are basically supported in neural processes of LTP and LTD. For example, LTP is produced when repeated transmissions or impulses through synapses of the neurons produce an effect of positive feedback amongst themselves, easing the execution of ulterior transmissions between those neural circuits that have been involved in such LTP [18].

The idea that memory is physiologically distributed in the brain seems to be a plausible and accepted assumption [19], [20]. Several aspects of memory have been analysed using different computational models [21]–[26], among others, the SDM [27]. SDM was developed as a mathematical model of long term human memory, where concepts in it are associated with patterns which that model must store.

These patterns can be stored by using points in a high dimensional space which act as storage addresses and which are randomly calculated. This random selection of points in space gives, as a result, points which are found to be sufficiently isolated and far from each other. These points act as storage indices of a representative part of the patterns that must be stored, so that the network stores the patterns in a distributed way. These storage indices would therefore be sufficiently far from each other, so that the indexing of the patterns is carried out in such a way that their recovery is appropriate [27]. This approach is somewhat related (or can be easily extrapolated) to the functioning of the brain and how the brain finally stores concepts.

In this context, we present a computational study whose objective is to see how the diffusion of NO can improve information storage and indexing. A classical architecture of associated memory such as the SDM is implemented, and in this we introduce the dynamic of diffusion of NO by means of a Model of Diffusion of NO based on Multi-compartmental Systems [28].

This work is organized into four main sections. The introduction places our objective into its context: a computational study of the implications of NO in neuro-indexing of the information in the BNN, as well as in classical SDM architecture.

The method section presents the NO dynamic model and the development of the Sparse Distributed Memory by NO Diffusion Model (SDM-NO). The methodology used to obtain the SDM-NO is based on the modification of the mechanism of indexing of the patterns that the SDM classical model stores, showing that this indexing depends on the NO dynamics.

The results section includes the development of this new model and compares it to the classical model for the different adjustment parameters that we have worked with: model size (k), Kanerva radius (ρ) and the workload that the model was subjected to (q). The study ends with a discussion of the results followed by our conclusions.

II. METHOD

The current understanding of the relationship between nerve cells which affect brain activity establishes a connection of classical synaptic neurotransmission and the confluence of cellular signals from different sources. These cellular signals include the processes of diffusion of different chemical substances in the nervous tissue and their follow up reactions, leading to the emergence of Volumetric Transmission (VT), which carries out a type of complex (not simple) communication, at short and long distances. The diffusion of neuroactive substances such as NO, CO or H_2S are underlying mechanisms in the extracellular space, which acts as a reduced environment for the separation of nerve cells and also serve as a channel of information amongst each other [29] and [30]. Even though these substances belong to the most toxic group known to us, they are present in numerous organisms (from bacteria up to human beings), carrying out signaling functions and information transmission [8]. NO carries out VT with proven implication in LTP, in such a way that the absence of NO does not produce LTP [15], [31]. Thus, NO is involved in the changes that underline learning and memory formation. Therefore NO diffusion will be the subject of this work.

We will analyse how the NO dynamics can influence the formation of memories and the information indexing of the BNN. We use a Compartment based NO Diffusion Model [28], to introduce the NO dynamics in the mechanism of information indexing that the SDM carries out.

A. NITRIC OXIDE DYNAMIC AS VOLUME SIGNAL

NO acts as an atypical neurotransmitter whose dynamic is formed by a set of specific processes:

- NO *Generation* or *Synthesis* is functionally required in the neural activity and begins by presynaptic release of glutamic acid [12], which combines with the NMDA receptors (N-methyl-d-aspartate), AMPA/kainate and metabotropic, forcing the entry of Calcium (Ca^{2+})

to the postsynaptic element where the activation of the Calmodulin produces NO Synthase enzyme (NOS) and activates different protein compounds [32]–[34]. Amongst said proteins calmodulin (CaM), together with Ca^{2+} and NOS facilitate the oxidation of L-arginine to synthesize citrulline and NO, causing a rapid and transitory release of moderate quantities of NO that diffuse in all directions before reaching the presynaptic neuron. It is there that it recombines with different substances and adjusts the release of neurotransmitters such as acetylcholine, aspartate or glutamic acid generating a loop in the synaptic signaling, since the activation process in the postsynaptic cell possesses a greater influence in its own process than the one activated in the presynaptic one (see figure 1).

This generation process is not local; it is conditioned only by the existence of the NOS enzyme and the flow of Ca^{2+} unlike the classic neurotransmitter, which is restricted by the synaptic terminals.

- NO *Diffusion* is moderated by the gradient of its own concentration. As opposed to the classic neurotransmitter, NO freely diffuses along with and around neural tissue and it is permeable membrane, and is able to move in its diffusion process up to 300 μm, reaching $2 \cdot 10^6$ synapses [8], influencing those cells that have appropriate receptors such as the Soluble Guanylyl Cyclase (sGC) enzyme [12], [35]. Along this line, NO does not act consistently with the Dynamic Polarization law of Cajal [36], since the information transfer is not carried out in one direction in the synapsis, but instead three dimensionally in all directions (Volume Transmission).
- The NO is able to *self-regulate* its production, using its contribution to inhibit NOS activity by a negative retroaction mechanism, leaving the area in a period of refraction, during which time it cannot return to produce NO synthesis. It also recombines with different substrates [37]. These processes are another difference that NO reveals with conventional neurotransmitters.

Consequently, modeling the dynamics of NO implies gathering each and every one of its processes in the model: *synthesis* or generation, *diffusion*, and *self-regulation*, with independence of the type of environment which is producing these dynamics, and for which we will use a nonlinear compartamental dynamical system model [39], [40].

The NO Diffusion Model based on Multi-compartmental Systems [28], which is used in this computational study, is a discrete model that defines space by means of discrete elements of volume, called compartments. These compartments have associated individual concentrations C_i of NO, and it is where any of the processes that make up the NO dynamics can take place. Figure 2 shows the framework in a mono-dimensional environment.

The *synthesis* process of NO is represented by the function F_i, which defines the quantity of NO that is created in this process, just like the profile of this generation of NO over time. As a result, when $F_i > 0$, there is a process of synthesis of NO in the compartment i and it is generating new NO, and when $F_i = 0$ in that compartment there is no synthesis process.

The *diffusion* process is based on transport phenomena; where these last ones determine which must move from the compartments of larger concentration to those of lower concentration. It can be inferred that the speed of the NO flow between two compartments is proportional to the difference of NO concentration between both compartments.

Finally, the variation of the NO concentration in a compartment is influenced by the *self-regulation* of the substance $(-\lambda_i C_i)$.

The NO dynamic is expressed, from a mathematical perspective, by means of equation 1, which corresponds to equation of mass balance of our compartments Model. We can see how the different processes (*synthesis*, *diffusion* and *self-regulation*) are influencing the dynamics of nitric oxide. The expression shows how the three different aforementioned processes are involved in the NO dynamic.

$$\frac{dC_i}{dt} = F_i + D_{i,i-1}(C_{i-1} - C_i) + D_{i,i+1}(C_{i+1} - C_i) - \lambda_i C_i \tag{1}$$

where $D_{i,i-1}$ and $D_{i,i+1}$ are the coefficients of diffusion between the compartments i and $i-1$ and between i and $i+1$ respectively. λ_i is the NO self-regulation coefficient, considering that said self-regulation is proportional to concentration [28].

The global behavior of the system and, consequently, the diffusion model of NO in a mono-dimensional environment is given by a system of N interrelated equations amongst themselves with existent boundary conditions.There are two following conditions:

1) *Non-cyclical boundary conditions*. The variation of the concentration in the compartments limits ($i = 1$ and $i = N$) only depend on the NO dynamics that is generated in them and in the neighboring compartments, according to the linear layout of the compartments (compartment $i = 2$ and compartment $i = N - 1$).
2) *Cyclical boundary conditions*. In this case, the compartments located in the limits ($i = 1$ and $i = N$) are connected to each other, where then the neighboring compartments of compartment $i = 1$ are compartments $i = 2$ and $i = N$, and from compartment $i = N$ compartments $i = N - 1$ and $i = 1$.

This way, the model is defined by a system of first order differential equations (equation 2).

$$\frac{dC}{dt} = HC + F, \tag{2}$$

where $C = (C_1, C_2, \ldots, C_N)^T$, $F = (F_1, F_2, \ldots, F_N)^T$, and for the case of conditions of cyclical surrounding, we have

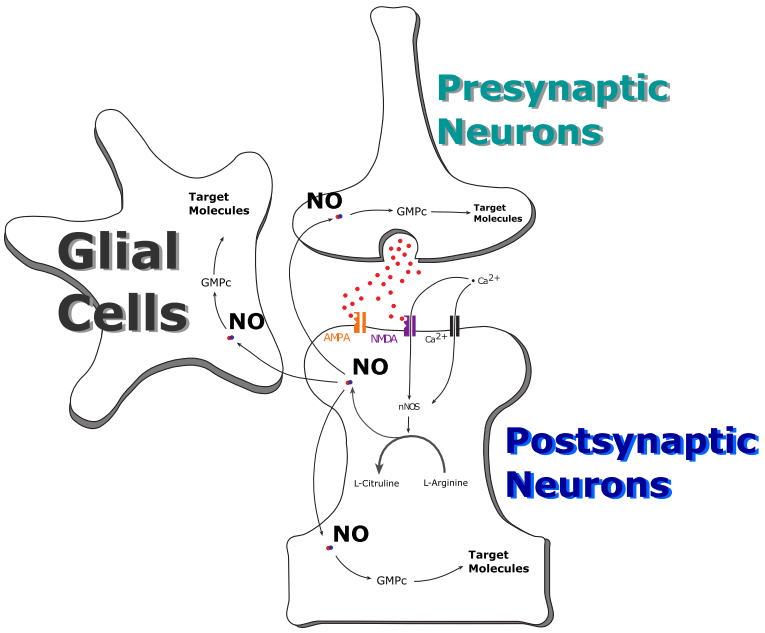

FIGURE 1. NO as a retrograde cellular messenger in CNS. Adapted from [38].

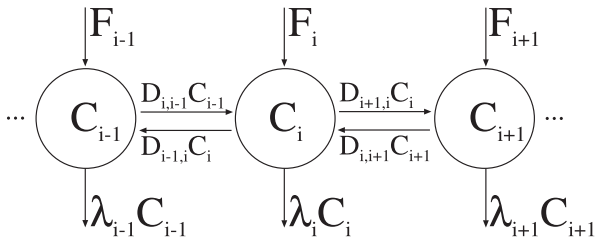

FIGURE 2. Mono-dimensional environment of compartments for the NO dynamics.

the following expression for H (tridiagonal matrix).

$$\begin{pmatrix} -(D_{1,N}+D_{1,2}+\lambda_1) & D & \dots \\ D & -(D_{2,1}+D_{2,3}+\lambda_2) & \dots \\ \vdots & \vdots & \ddots \end{pmatrix} \quad (3)$$

Which in environments with completely isotropic and homogeneous features $D_{i,j} = D_{j,i}, \forall i, j$ and $\lambda_i = \lambda_j, \forall i, j$, provide a direct solution. The former model for a mono-dimensional environment, made up of N compartments, can be tended for bidimensional and three dimensional environments like those used in this work, which would be in function of the way in how we define the diffusion space, explained in section II-C.

B. SPARSE DISTRIBUTED MEMORY MODEL

Sparse distributed memory (SDM) [27] is considered a variation of Random Access Memory (RAM), and it is a model of associated memory that is made up of two main components (address matrix Q and memory matrix M) (see figure 3). SDM is characterized by the following features:

- Instead of addressing to a single memory address, the SDM calculates the corresponding distance between the set address and all configured addresses in its address matrix Q. When all these distances have been calculated, the registers of memory M, whose distance is less than the set Radius value, are activated.
- Storage is carried out by adding $+1$ in the positions of all registers of M that have been activated, if and only if the value that is stored in said position is equal to 1. Otherwise -1 is added.
- Gathering a stored datum is carried out by performing a series of operations with the registers of M that are activated. First, for each position, all registers in an active state are added up. If the sum for each position is greater than or equal to zero, the recovered register then has a 1 in this position; otherwise, 0.

In order to understand the procedure of learning and recovery of patterns in the SDM we must consider the set $A = \{0, 1\}$ being worked on, in addition to the set made up of p pairs of elements $(x^\mu, y^\mu) \in (A^n, A^m)$ where $\mu = 1..p$.

Two steps are needed before proceeding to the Learning and Recovery Phases. They are:

1) Choose a value for k that satisfies $n \ll k \ll 2n$. This value is the number of physical storage registers in the memory.
2) A $Q_{k\times n}$ matrix, whose elements are $q_{ij} \in A$, is randomly calculated.

The learning phase is made up of two stages. In the first stage, each one of the p associations (x^μ, y^μ) is carried out in the following steps:

FIGURE 3. SDM scheme which stores m-bit registers.

a) Calculate the Hamming distance vector $h^\mu = Q_{x\times n} \otimes x^\mu$, where the operation $\otimes$ is defined as follows:

$$h_i^\mu = \sum_{j=1}^{n} q_{ij} \oplus x_j^\mu. \tag{4}$$

where $i = 1..k$ and $\mu = 1..p$, and consequently the stored values in the input of vector h^μ are integers between 1 and n.

b) A Kanerva radius ρ is chosen. It must be a number in the range $n/2 \geq \rho \geq 1$.

c) The internal transition column vector b^μ, is calculated, with dimension k, and whose i^{th} component is computed using the following expression:

$$b_i^\mu = \begin{cases} 1 \ if \ h_i^\mu \leq \rho \\ 0 \ otherwise \end{cases} \tag{5}$$

where $i = 1..k$ and $\mu = 1..p$.

d) Calculate M^μ matrix, with dimensions $k \times m$, according to the following:

$$m_{ij}^\mu = \begin{cases} 1 \quad if \ (b_i^\mu = 1) \wedge (y_j^\mu = 1) \\ -1 \ if \ (b_i^\mu = 1) \wedge (y_j^\mu = 0) \\ 0 \qquad otherwise \end{cases} \tag{6}$$

where $i = 1..k, j = 1..m$ and $\mu = 1..p$. This calculation is the same as performing the following operations with vectors y^μ and b^μ:

$$m_{ij}^\mu = (2y_j^\mu b_i^\mu - 1)b_i^\mu. \tag{7}$$

The second stage in the Learning phase deals with the addition operations of the p calculated matrices M^μ from the first stage. Consequently, we calculate M by means of the following expression:

$$M = \sum_{\mu=1}^{p} M^\mu. \tag{8}$$

The Recovery phase is also made up of two stages, starting with input pattern e^ω, where $\omega = 1..p$ if the noise level equals zero then $e^\omega = x^\omega$. The steps of the first stage are:

a) Calculate the Hamming distance vector $h^\omega = Q_{k\times n} \otimes e^\omega$, where, in this case the operation ω is defined from the following:

$$h_i^\omega = \sum_{j=1}^{n} q_{ij} \oplus e_j^\omega. \tag{9}$$

where $i = 1..k$ and $\omega = 1..p$.

b) Calculate the internal transition column vector b^ω, with dimension k, and whose i^{th} component is calculated using the following expression:

$$b_i^\omega = \begin{cases} 1 \ if \ h_i^\omega \leq \rho \\ 0 \ otherwise \end{cases} \tag{10}$$

where $i = 1..k$ and $\omega = 1..p$.

There are three steps in the second stage:

a) The m representative thresholds are calculated in the vector θ^ω, whose i^{th} component is calculated using the following expression:

$$\theta_j^\omega = \frac{1}{2} \sum_{i=1}^{k} m_{ij}. \tag{11}$$

where $i = 1..k, j = 1..m$ and $\omega = 1..p$.

b) Get a second internal transition column vector t^{ω} with dimension m, whose i^{th} component is calculated using the following expression:

$$t_j^{\omega} = \sum_{i=1}^{k} m_{ij} b_i^{\omega}. \tag{12}$$

where $i = 1..k, j = 1..m$ and $\omega = 1..p$.

c) Finally the output of the SDM s^{ω}, of m dimensions, is obtained, which corresponds to the best recovery from the memory of the pattern stored y^{ω}. The calculation of s^{ω} is carried out using the following expression:

$$s_j^{\omega} = \begin{cases} 1 \ if \ t_j^{\omega} \geq \theta_j^{\omega} \\ 0 \ \ otherwise \end{cases} \tag{13}$$

where $j = 1..m$ and $\omega = 1..p$.

Modifying the calculation of the threshold vector θ^{ω} setting the previous vector 0 equal to the zero vector for all ω, allows us to establish a variation of the SDM model in its Recovery Method.

C. SPARSE DISTRIBUTED MEMORY MODEL BY DIFFUSION

The difference between our SDM by diffusion model (SDM-NO) and the classic SDM model is in the consideration of the NO diffusion dynamic in the construction of the Q matrix. Our aim is to compare the way in which the NO diffusion indexes information in matrix M, to how it is randomly done when the SDM model is used. Figure 4 presents a schematic of our modified version of the SDM.

The Q generator considering NO diffusion is constructed using the following:

We define a diffusion space in direct relation with the concept of distance between the elements $x^{\mu} \in A^n$. This diffusion space Δ_n will be made up of a set of compartments $\{C_j\}$, where each compartment has an associated bitmask m_j that is built on the set $\{\bullet, 1\}^n$, where $\bullet$ represents the possibility that there is either a 1 or a 0 in the position where it is found. There is also an integer $1 < i < n$ associated with each compartment which quantifies the number of $1's$ found in m_j.

We can then proceed to define the diffusion space when $n = 3$ in the following way: $\Delta_3 = \{C_1, C_2, C_3, C_4, C_5, C_6\}$ and with the following set of associated masks $\{m_1 = 1 \bullet \bullet, m_2 = \bullet 1 \bullet, m_3 = \bullet \bullet 1, m_4 = 11\bullet, m_5 = 1 \bullet 1, m_6 = \bullet 11\}$. Similarly we arrive to $\Delta_4 = \{C_1, C_2, C_3, C_4, C_5, C_6, C_7, C_8, C_9, C_{10}, C_{11}, C_{12}, C_{13}, C_{14}\}$ and its set of associated bitmasks $\{m_1 = 1 \bullet \bullet\bullet, m_2 = \bullet 1 \bullet \bullet, m_3 = \bullet \bullet 1\bullet, m_4 = \bullet \bullet \bullet 1, m_5 = 11 \bullet \bullet, m_6 = 1 \bullet 1\bullet, m_7 = 1 \bullet \bullet 1, m_8 = \bullet 11\bullet, m_9 = \bullet 1 \bullet 1, m_{10} = \bullet \bullet 11, m_{11} = 111\bullet, m_{12} = 11 \bullet 1, m_{13} = 1 \bullet 11, m_{14} = \bullet 111\}$ and successively for any n > 4.

The distance definition [27] can be extended to collect the distance between the two bitmasks, since we will define the connectivity between the two compartments as a function of this concept.

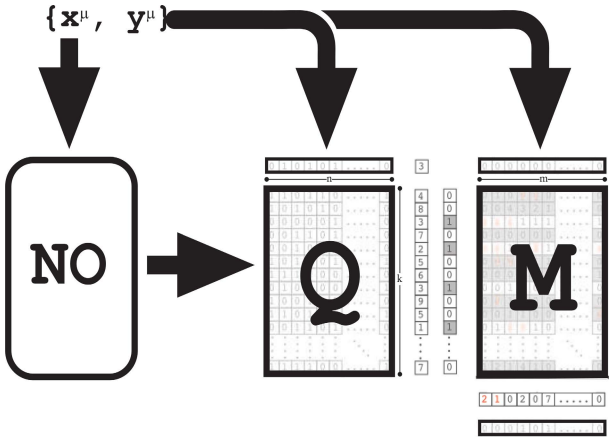

FIGURE 4. SDM schematic that stores *m* bit registers, where the calculation of the *Q* matrix is carried out based on the diffusion dynamic.

TABLE 1. Distances between each pair of involved masks in the diffusion space Δ_3.

	$m_1(100)$	$m_2(010)$	$m_3(001)$	$m_4(110)$	$m_5(101)$	$m_6(011)$
$m_1(100)$	0	2	2	1	1	3
$m_2(010)$		0	2	1	3	1
$m_3(001)$			0	3	1	1
$m_4(110)$				0	2	2
$m_5(101)$					0	2
$m_6(011)$						0

Given any two bitmasks m_j and m_k, which are associated to two compartments C_j and $C_k \in \Delta_n$, we define the distance $d(m_j, m_k)$ between them as the distance that exists between the two defined patterns by m_j and m_k when we set $\bullet = 0$. Table 1 shows the calculation of the distances for Δ_3.

Using the previous definition of distance between bitmasks, we establish that two compartments C_j and C_k are connected if their associated bitmasks satisfy that $d(m_j, m_k) = 1$. This allows us to establish the diffusion space for any value of n. Figures 5 and 6 show the diffusion spaces for $n = 3$ and $n = 4$ respectively.

The diffusion dynamic takes place in this space and allows us to construct a Q matrix following the modified probabilities in the q_{ij}. These probabilities change as a function of the influences they have on the associated compartments in that diffusion space and the influences that these compartments have on the probabilities.

The above constructs a Q matrix, showing the probability of the possible addressing vectors of the matrix as a function of the diffusion dynamics which has taken place in its associated compartment. For example, for a SDM-NO model with $n = 3$, we have seen that the diffusion space Δ_3 we are working with is made up of 6 compartments, whose diffusion dynamics will define the probability of the different addressing vectors that are present in the Q matrix in the following way:

Compartment C_1 has as associated bitmask $m_1 = 1 \bullet \bullet$, and the probability that the directionality vector 100 is found in Q is $f_1(c_1^{max}, c_2^{max}, c_3^{max}, c_4^{max}, c_5^{max}, c_6^{max})$, where c_1^{max}, $c_2^{max}, c_3^{max}, c_4^{max}, c_5^{max}, c_6^{max}$ correspond to the maximum

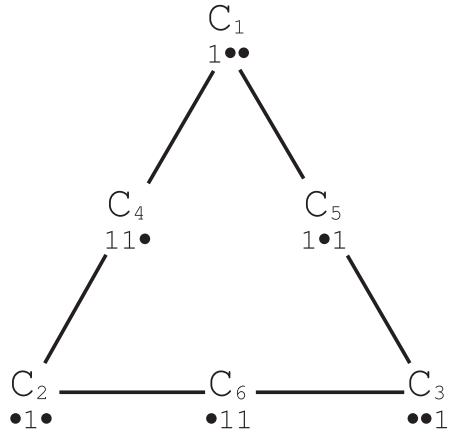

FIGURE 5. Diffusion space Δ_3.

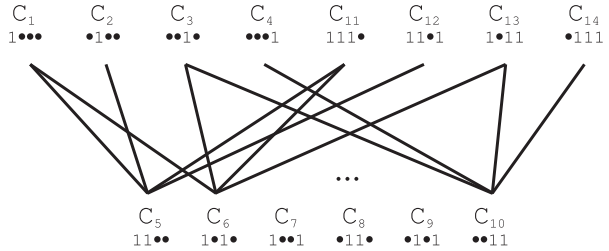

FIGURE 6. Diffusion space Δ_4.

concentration of NO reached in said compartments and f_1 is an orthogonality function of c_1^{max} on the remaining maximum concentrations reached in the other compartments. In a similar way we can calculate the probabilities of the different addressing vectors associated to the bitmasks of each compartment.

This process of calculation of probabilities of the different addressing vectors is easily extended for any value of n, and does not always fix a value of associated probability to the addressing vectors that force them to be included in the Q matrix.

Lastly, the fact that the size k of the memory always is smaller than the number of compartments that constitutes the diffusion space must also be considered.

III. RESULTS

Our initial hypothesis under study is that NO diffusion dynamic could improve the way in which Sparse Distributed Memory indexes information in its learning phase. A computational study on indexing information is carried out and serves as the starting point of our formal study.

No structural modification of the model is aimed. *Indexing information* refers to how the SDM network internally locates patterns. In classic SDM, this location has important consequences in the final functionality, since it must minimize overlap of stored patterns (x^μ, y^μ), in proportion to the value displayed in the Kanerva radius ρ. Our comparative study uses 8 bit memories: a classic 8 bit SDM and an 8 bit SDM-NO memory. We identify the following working variables to analyse the behavior of both models:

- *Network size*, (k) is given by the size of that part of the network responsible for the addressing of the patterns.
- *Network workload*, (q) is the number of stored patterns in the network.
- *Kanerva radius* (ρ), is one of the functional parameters of the network, with implications for the directionality dynamics of the network.
- *Network performance* (ζ) is the recovery capacity of the network, in accordance to what is stored.

Given these considerations, we analyse the performance of memories when we store and recover 8 bit randomly generated binary patterns and then use them as inputs for both networks. We focus on the ability to recover stored patterns in a functionality state where the network workload exceeds the network size.

The concept of capacity in our SDM-NO model must be handled with caution. Asymptotic behavior of the ability of the SDM model has been studied from different perspectives [41]–[43]. This capacity is related with the ability of the model to recover a stored pattern (assuming a specified degree of accuracy) when we request a readout in which we use addressing patterns close to the addressing pattern with which it was stored. This situation is strongly related with the tolerance of the model to noise found in the stored patterns and which are used in the recovery process.

As mentioned previously, our study focuses on the concept of indexing, showing its relationship with the Q matrix and the way in which it is generated. To do so we have used a definition of ζ (network performance) requiring complete recovery of patterns without analyzing if the SDM-NO model has modified its noise tolerance.

Figures 7 to 14 present a comparison of both memories using different network sizes. These figures always show the network performance (ζ) as a function of network workload (q) and Kanerva radius ρ, when studying different network sizes (k and n).

Network performance values ζ throughout the study have been in the range (0, 1), where value of 0 means the network was unable to recover any stored pattern and the value of 1 revealed that the network was able to recover all stored patterns. The approach was applied to different sizes k of the model to store a number of patterns which was greater than the model size.

Figure 7 shows us models performance as a function of the Kanerva radius (ρ) and the network workload. By focusing on the basic recovery method (figure 7a), which fixes average values for the thresholds θ^ω, a minimized generalized performance is revealed in both networks for all values in all parameters, suggesting that both, SDM and SDM-NO model, when the Kanerva radius $\rho = 1$, and independently of network workload, is unable to recover the stored patterns in it. When the radius ρ increases, an improvement in performance is observed, reaching a recovery rate of approximately 20% when the Kanerva radius values are $\rho = 3$ or $\rho = 4$.

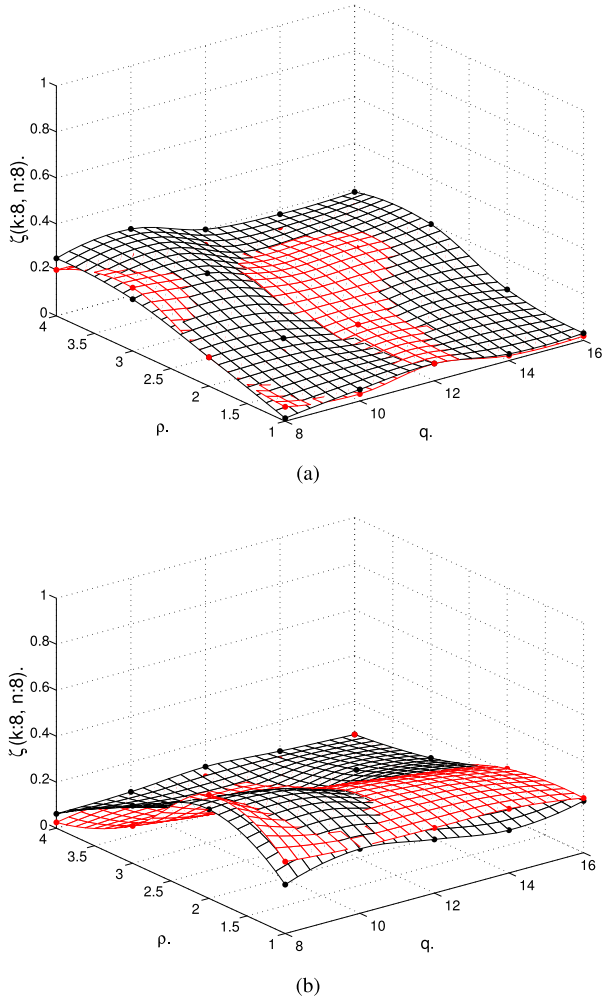

FIGURE 7. Models performance (SDM black and SDM-NO red) for size $k = 8$, as a function of Kanerva radius ρ and the network workload q. (a) Basic pattern recovery method and (b) Model using $\theta^{\omega} = 0$.

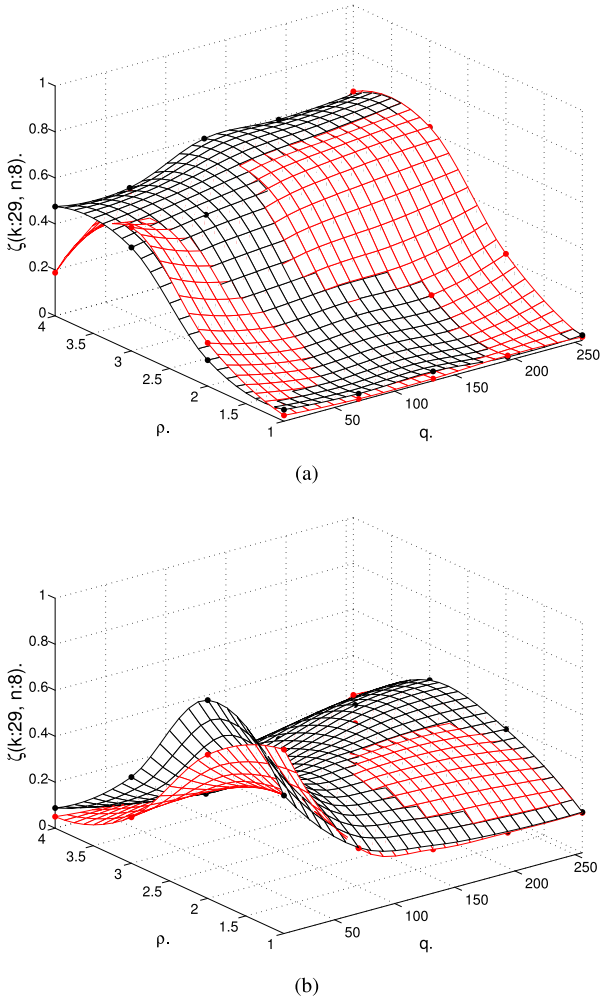

FIGURE 8. Graph of model performance (SDM black and SDM-NO red) for size $k = 29$, as a function of Kanerva radius ρ and the network workload (a) Basic pattern recovery method and (b) Model with $\theta^{\omega} = 0$.

And yet the same figure 7a allows us to see how the behavior of the SDM-NO network slightly improves the SDM network for values of $\rho = 1$ to 3 and half workload, and for values of $\rho = 3$ and minimum network workload, as noted in the areas where the surface corresponding to SDM-NO is greater than that of the SDM.

The behavior of models when null thresholds $\theta^{\omega} = 0$ are used is similar to those commented previously, showing an apparent inversion with regards to the values of ρ where the network seems intent on improving functionality or performance (see figure 7b).

Figures 8, 9 and 10, show model performance for network sizes that increase from $k = 29$ up to $k = 116$. We can observe that networks improve their recovery ability to what has been stored based on increase in size. In these figures two types of recovery methods are also displayed, with clear differences depending on the values of θ^{ω}: average values (subfigures 8a, 9a and 10a) and null values (8b, 9b and 10b). The behavior of both methods is confirmed to reflect opposite performance. The first method offers better evidence of functionality for high values of the Kanerva radius, while the second one reveals the opposite.

All results from this analysis have been confirmed by means of a quantitative study using two different kinds of patterns:

a) Random binary string with 8 bits,
b) Binary images of handwritten alphabet characters with a dimension 10×10.

We will study the number of patterns that can be completely recovered by both SDM and SDM-NO architectures when they work with prior pattern types. When pattern type is from set a), we use a network size of $k = 116$ with different workload values q within the interval $[max(k/2, n), min(2k, 2^n)]$. Obtained results for a ρ value varying from 1 to $n/2$ can be seen in table 2. The best behaviour in both models is obtained when $\rho = 3$. Thus, when both networks are subject to $q = 232$ patterns, practically all those stored are recovered (217 for SDM network and 225 for the SDM-NO network). These results confirm the obtained performance profiles, see figures 9 and 10.

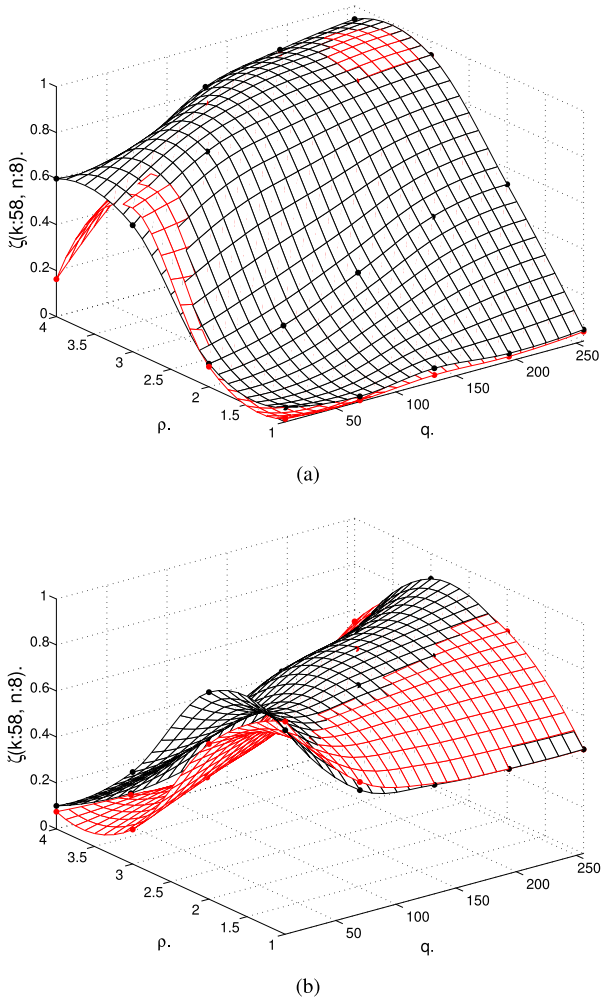

FIGURE 9. Models performance (SDM black and SDM-NO red) for size $k = 58$, as a function of the Kanerva radius ρ and the network workload. (a) Basic pattern recovery method and (b) Model with $\theta^{\omega} = 0$.

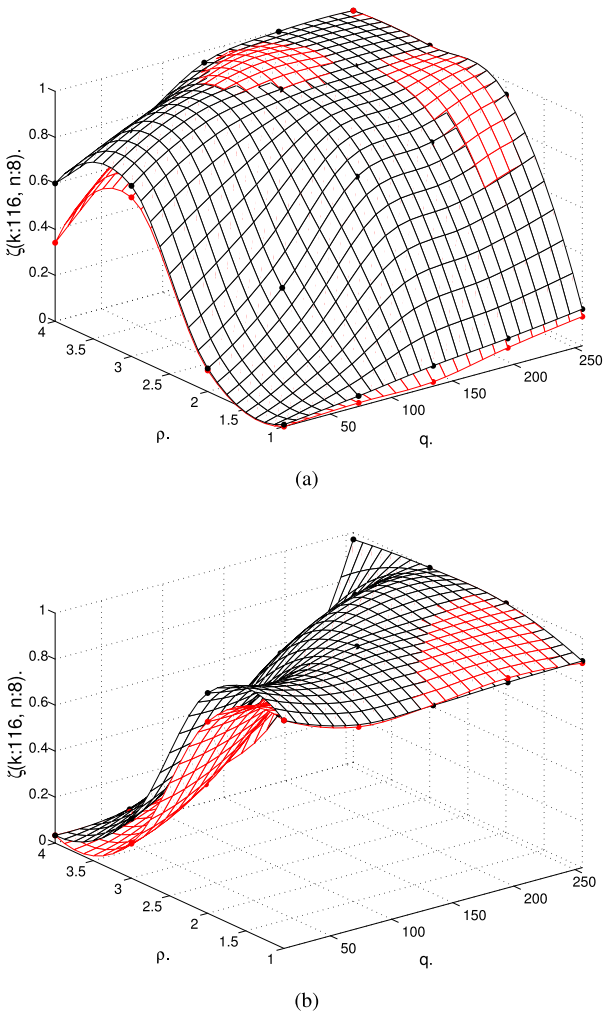

FIGURE 10. Models performance (SDM black SDM-NO red) size $k = 116$, as function of Kanerva radius ρ and the network workload. (a) Basic pattern recovery method (b) Model with $\theta^{\omega} = 0$.

TABLE 2. The number of completely recovered patterns from the SDM and SDM-NO networks, using random binary patterns of $n = 8$ bits and $k = 116$.

	$q = 58$	$q = 87$	$q = 116$	$q = 174$	$q = 232$
$\rho = 1$	2/1	3/1	3/2	9/5	11/5
$\rho = 2$	16/9	23/13	32/21	65/48	105/78
$\rho = 3$	45/45	70/73	102/105	163/163	217/225
$\rho = 4$	37/35	61/57	91/89	146/154	201/208

Figure 11 shows how the $\zeta(n = 8, k = 116, \rho = 3)$ function behaves as q increases. Note that both network models reveal better performance values, almost at 100% (all the stored patterns have been completely recovered) for workload values q that exceed the network size, $q \gg k$. Low q workload values, $q \ll k$, reveal performance levels around 88% for the SDM network and 86% for the SDM-NO network. When q and k are practically equal $q \cong k$, both models perform at a very high 95% level. A review of obtained results reveals that the SDM-NO network model performs practically the same as the traditional SDM network model.

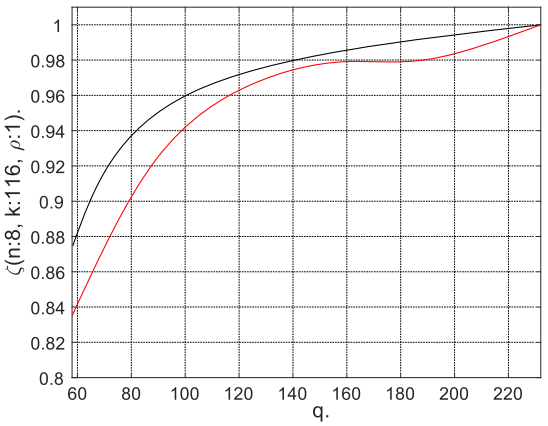

FIGURE 11. Network comparison (SDM in blue, SDM-NO in red), according to their total recovery capacities.

We finally confirm the previously mentioned analysis of our results using the type b) set of patterns. To do so we used the following parameter values in the configuration of both

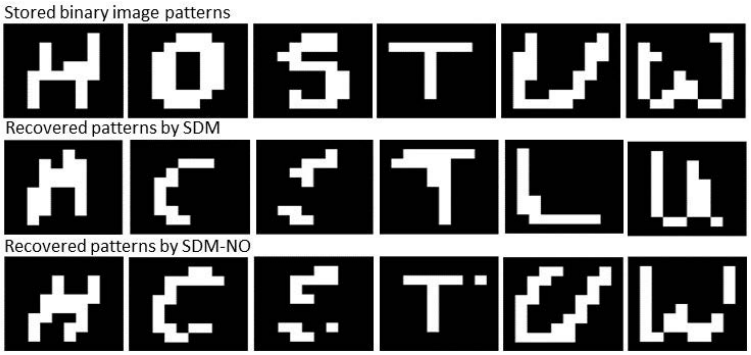

FIGURE 12. Results belonging to recovery of some handwritten characters patterns by the two neural architectures, SDM and SDM-NO.

TABLE 3. Number of binary image patterns, handwritten characters, with $n = 100$ bits and $k = 9902$, that are completely recovered by SDM and SDM-NO networks.

	4951	7427	9902	14853	19804
P^{R}_{SDM}	5	8	2	1	0
P^{NR}_{SDM}	4946	7419	9900	14852	19804
P^{R}_{SDM-NO}	3	10	1	1	0
P^{NR}_{SDM-NO}	4948	7417	9901	14852	19804

models:

- Pattern size, $n = 100$ bits,
- network size $k = 9902$,
- and $\rho = 49$,

Network workload q takes on the following values: $q = \{4951, 7427, 9902, 14853, 19804\}$, allowing low workloads, covering half of the network size, as well as high workloads, which is twice the size of the network.

Upon completion of the storage of pattern set stage for both studied SDM network models, the recovered patterns by each of the two SDM models, are summarized in table 3, using the following nomenclature:

- P^{R}_{SDM}: completely recovered patterns from the SDM network.
- P^{NR}_{SDM}: partially recovered patterns from the SDM network.
- P^{R}_{SDM-NO}: completely recovered patterns from the SDM-NO network.
- P^{NR}_{SDM-NO}: partially recovered patterns from the SDM-NO network.

Complete recovery means that the neural architectures have been able to recover the exact stored pattern (recovered value for each image pixel is exactly the same as the stored value for that pixel).

We can observe in Table 3 that both neural architectures, SDM and SDM-NO, are able to obtain only a very small number of whole recovered binary image patterns. Figure 12 shows the results for recovery of different binary

TABLE 4. Percentage of zero and one pixels corresponding the handwritten character images which were completely recovered by both networks and for different network workloads q.

	4951	7427	9902	14853	19804
$\%0\ SDM$	98%	98%	98%	98%	98%
$\%0\ SDM-NO$	96%	97%	96%	97%	96%
$\%1\ SDM$	17%	14%	14%	14%	17%
$\%1\ SDM-NO$	34%	32%	32%	31%	32%

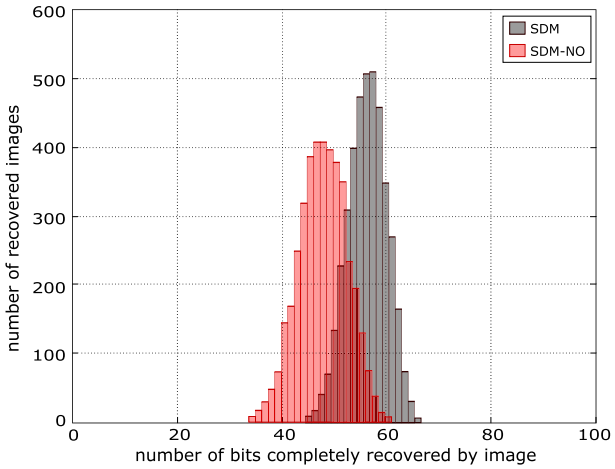

FIGURE 13. Comparative histogram of the recovery process for both models, Kanerva (SDM) and our proposal (SDM-NO).

image patterns performed by the two models of sparse distributed memory. Note that in neither case are the images that were previously stored are completely recovered. However, a visual review indicates that the performance by the SDM-NO model is superior to the one by the SDM (Kanerva) model.

More specific details of the recovery process by both models can be obtained by means of an analysis of the percentage of correctly recovered ones and zeros in the stored patterns. These results as a function of workload q are shown in table 4. Notice that, with regards to recovery of ones, that SDM-NO network is superior to the SDM network. When compared to column for a $q = 4951$ workload, on average the SDM-NO network recovers 34% of the ones (active bits)

from the stored/original image, as opposed to 17% from the traditional SDM network. A review of the results for the recovery of zeros, however, is not the same. Both network models perform at approximately the same level, 96% for the SDM-NO network and 98% for the SDM network.

Figure 13 displays a comparison of the recovery process carried out by both neural network models using histograms that relate the number of recovered images (y axis) with number of bits completely recovered by image (x axis). The histograms reveals that the SDM-NO network recovered more than 400 images where the image coincided with the previously stored image in 49..50 bits. This result and those shown in figure 12 and table 4 identify the importance of recovery of those bits which contain the greatest amount of information. Our proposed SDM-NO network model is more effectively at acquiring this characteristic.

IV. DISCUSSION AND CONCLUSION

Obtained results from the Study and previous explanations provided in the results section not only reveal different behaviour and different capacity of information recovery by the SDM network of Kanerva and our proposed SDM-NO network, but it has also shown the different capacities of the models when using different information environments (random binary patterns versus binary images of handwritten characters).

Results associated with 8 bit randomly binary patterns suggest that studied variability in ρ (Kanerva radius) seems to induce a similar asymptotical behaviour in the performance of both SDM and SDM-NO models when working with this type of information environment.

The performance of the basic recovery method is generally superior to the recovery method $\theta^{\omega} = 0$, and it is in this latter method where the greatest differences between the SDM model and the SDM-NO model can be seen throughout all of the variability of ρ and when they are subject to the low workload of storage (close to network size).

The SDM-NO network with basic recovery method performs best when ρ is near 3, however when using high values, such as those approaching the limit $n/2$, its performance declines. The behavior of this same model is exactly the opposite when using half storage workload: the SDM-NO model shows better performance. Nonetheless, this improvement is minor with respect to the SDM with basic recovery method. Thus, it seems as if NO dynamics attain greater indexing of the patterns in high values of ρ but not approaching the limit of $n/2$, and when they are in half storage workload.

The SDM-NO with recovery method $\theta^{\omega} = 0$, and regarding the variability of ρ, presents an opposite behavior to the basic recovery method: best improvements occur with low values of ρ, whereas worst occur at high values. Even though there are clear differences between this model, which incorporates NO dynamics, and its counterpart SDM, both with the same recovery method, the asymptotical behavior of its performance, is similar in a low storage workload scenario.

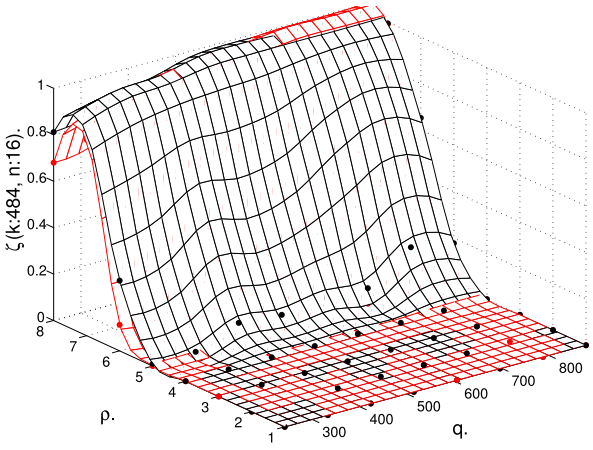

FIGURE 14. Performance of SDM model (black) and SDM-NO model (red)) for size $k = 484$, as a function of Kanerva radius ρ and for the network workload. Basic pattern recovery method.

This type of performance is typical and to be expected, since the way patterns are indexed in the network is the same for both recovery methods independently of the used recovery method.

The study has allowed us to identify the parametric intervals where models perform best. These ranges of values were used in the study, and we tested the models with a set of non-random patterns (handwritten letters), formed by binary 100 bit images (10×10 dimension) which allowed both neural network architectures to tackle problems that approximate real cases.

We have observed that the levels of complete pattern recovery for both network models are not very high. Almost all of the patterns end up being catalogued in the partial recovered subset P_*^{NR}, and the number of correctly recovered bits in the images for both models is found to be between 50..55%.

The detailed analysis of recovery by bit typology reveals that the SDM-NO network is better at recovery for areas of images that contain greater amounts of information. Results obtained are independent of workload q, and the SDM-NO network model displays the same proportion of correctly recovered bits (with greater information input) for lower workload values (half of network workload) as well as for higher workloads (double network size).

As regards indexing capacity we can conclude that the new model with its underlying mechanism in the NO diffusion dynamics shows similar behaviour to the randomly indexing network model.

A review of the different information settings used by the proposed SDM architecture and its behavior with the NO diffusion dynamic indexing mechanism shows satisfactory levels of complete pattern recovery and a slight improvement on increasing pattern sizes, figure 14, although this is not the case when working with handwritten characters, where the complete pattern recovery level is close to 0%.

In conclusion, recapping what was previously stated the indexing carried out by the SDM-NO model is quite similar

to the indexing performed by the SDM model, showing such indexing a dependence on the structural features of the information environment where both models are working.

Consequently, this computational study allows us to conclude that the NO diffusion dynamics model presents acceptable abilities to index information in the artificial SDM model, improving the indexing when compared to those carried out by randomly generated directionality patterns, since indexing capacity and its capacity for information recovery is practically the same in both models when working with random information in structured information settings which reflect real applications, and when the NO diffusion dynamic generates better indexing and recovery.

Finally, this work is the first step studying the asymptotic behaviour of the SDM-NO model capacity and its relation with the tolerance to the noise of the stored patterns. In future works we will also analyse the possible influence of others NO diffusion aspects and mechanisms on the SDM-NO model performance (ζ).

REFERENCES

[1] L. J. Ignarro, G. M. Buga, K. S. Wood, R. E. Byrns, and G. Chaudhuri, "Endothelium-derived relaxing factor produced and released from artery and vein is nitric oxide," *Proc. Nat. Acad. Sci. USA*, vol. 84, no. 24, pp. 9265–9269, Dec. 1987.

[2] S. Moncada, R. M. Palmer, and R. J. Gryglewski, "Mechanism of action of some inhibitors of endothelium-derived relaxing factor," *Proc. Nat. Acad. Sci. USA*, vol. 83, no. 23, pp. 9164–9168, Dec. 1986.

[3] R. M. J. Palmer, A. G. Ferrige, and S. Moncada, "Nitric oxide release accounts for the biological activity of endothelium-derived relaxing factor," *Nature*, vol. 327, no. 6122, pp. 524–526, Jun. 1987.

[4] M. T. Khan and R. F. Furchgott, "Additional evidence that endothelium-derived relaxing factor is nitric oxide," in *Pharmacology*, M. J. Rand and C. Raper, Eds. Amsterdam, The Netherlands: Elsevier, 1987, pp. 341–344.

[5] D. S. Bredt and S. H. Snyder, "Nitric oxide mediates glutamate-linked enhancement of cGMP levels in the cerebellum," *Proc. Nat. Acad. Sci. USA*, vol. 86, no. 22, pp. 9030–9033, Nov. 1989.

[6] D. S. Bredt, P. M. Hwang, and S. H. Snyder, "Localization of nitric oxide synthase indicating a neural role for nitric oxide," *Nature*, vol. 347, pp. 765–770, Oct. 1990.

[7] J. Garthwaite, G. Garthwaite, R. M. J. Palmer, and S. Moncada, "NMDA receptor activation induces nitric oxide synthesis from arginine in rat brain slices," *Eur. J. Pharmacol., Mol. Pharmacol.*, vol. 172, nos. 4–5, pp. 413–416, Oct. 1989.

[8] J. Herrmann, L. Lerman, and A. Lerman, "Simply say yes to NO? Nitric oxide (NO) sensor-based assessment of coronary endothelial function," *Eur. Heart J.*, vol. 31, no. 23, pp. 2834–2836, Dec. 2010.

[9] J. Regidor and C. P. S. Araujo, *Retrograde Neural Messenger in the Brain. Preliminary Study on the Implications in the Artificial Neural Networks. Brain Processes, Theories and Models*. Cambridge, MA, USA: MIT Press, 1995, pp. 360–369.

[10] C. P. S. Araujo, "Study and reflections on the functional and organizational role of neuromessenger nitric oxide in learning: An artificial and biological approach," *AIP Conf. Proc.*, vol. 517, no. 1, pp. 296–307, 2000.

[11] G. M. Edelman and J. A. Gally, "Nitric oxide: Linking space and time in the brain," *Proc. Nat. Acad. Sci. USA*, vol. 89, no. 24, pp. 11651–11652, Dec. 1992.

[12] J. Garthwaite and C. L. Boulton, "Nitric oxide signaling in the central nervous system," *Annu. Rev. Physiol.*, vol. 57, pp. 683–706, Mar. 1995.

[13] D. Centonze, P. Gubellini, G. Bernardi, and P. Calabresi, "Permissive role of interneurons in corticostriatal synaptic plasticity," *Brain Res. Rev.*, vol. 31, no. 1, pp. 1–5, Dec. 1999.

[14] H. Daniel, C. Levenes, and F. Crépel, "Cellular mechanisms of cerebellar LTD," *Trends Neurosci.*, vol. 21, no. 9, pp. 401–407, Sep. 1998.

[15] E. R. Kandel, "Genes, synapses, and long-term memory," *J. Cellular Physiol.*, vol. 173, no. 2, pp. 124–125, Nov. 1997.

[16] E. R. Kandel, *In Search of Memory: The Emergence of a New Science of Mind*. New York, NY, USA: W. W. Norton & Company, Mar. 2006.

[17] A. G. García, "La química y la mecánica de la comunicación neuronal," in *Ensayos Sobre Neurociencias*, F. Mora, Ed. Barcelona, España: Ariel, 1996, pp. 40–65.

[18] R. G. M. Morris, "Long-term potentiation and memory," *Philosophical Trans. Roy. Soc. London B, Biol. Sci.*, vol. 358, no. 1432, pp. 643–647, 2003.

[19] F. H. C. Crick and C. Asanuma, "Certain aspects of the anatomy and physiology of the cerebral cortex," in *Parallel Distributed Processing: Explorations in the Microstructure of Cognition* (Psychological and Biological Models), vol. 2. Cambridge, MA, USA: MIT Press, Nov. 1986, pp. 333–371.

[20] T. J. Sejnowski and C. R. Rosenberg, "NETtalk: A parallel network that learns to read aloud," Dept. Electr. Eng. Comput. Sci., Johns Hopkins Univ., Baltimore, MD, USA, Tech. Rep. JHU/EECS-86/01, 1986, p. 32.

[21] T. Kohonen, "Correlation matrix memories," *IEEE Trans. Comput.*, vol. C-21, no. 4, pp. 353–359, Apr. 1972.

[22] P. F. López, C. P. S. Araujo, P. G. Báez, and G. S. Martin, "Diffusion associative network: Diffusive hybrid neuromodulation and volume learning," in *Computational Methods in Neural Modeling* (Lecture Notes in Computer Science), vol. 2686, J. Mira and J. R. Álvarez, Eds. Giza, Egypt: IWAN, 2003, pp. 54–61.

[23] T. Kohonen, "Self-organized formation of topologically correct feature maps," *Biol. Cybern.*, vol. 43, pp. 59–69, Jan. 1982.

[24] J. J. Hopfield, "Neural networks and physical systems with emergent collective computational abilities," *Proc. Nat. Acad. Sci. USA*, vol. 79, no. 8, pp. 2554–2558, Apr. 1982.

[25] J. L. McClelland and D. E. Rumelhart, "Distributed memory and the representation of general and specific information," *J. Exp. Psychol., Gen.*, vol. 114, no. 2, pp. 159–188, 1985.

[26] M. Nakagawa, "On the entropy based associative memory model with higher-order correlations," *Entropy*, vol. 12, no. 1, pp. 136–147, Jan. 2010.

[27] P. Kanerva, *Sparse Distributed Memory*. Cambridge, MA, USA: MIT Press, 1988.

[28] C. P. S. Araujo, P. F. López, P. G. Báez, and J. L. S. D. Fonseca, "A model of nitric oxide diffusion based in compartmental systems," *Int. J. Comput. Anticipatory Syst.*, vol. 18, pp. 172–186, Jul. 2006.

[29] E. Syková, "The extracellular space in the CNS: Its regulation, volume and geometry in normal and pathological neuronal function," *Neuroscientist*, vol. 3, no. 1, pp. 28–41, Jan. 1997.

[30] E. Syková, "Extrasynaptic volume transmission and diffusion parameters of the extracellular space," *Neuroscience*, vol. 129, no. 4, pp. 861–876, 2004.

[31] J. Rodrigo, A. P. Fernández, J. Serrano, M. Monzón, E. Monleón, J. J. Badiola, S. Climent, R. Martínez-Murillo, and A. Martínez, "Distribution and expression pattern of the nitrergic system in the cerebellum of the sheep," *Neuroscience*, vol. 139, no. 3, pp. 889–898, Jan. 2006.

[32] H. W. Tao and M.-M. Poo, "Retrograde signaling at central synapses," *Proc. Nat. Acad. Sci. USA*, vol. 98, no. 20, pp. 11009–11015, 2001.

[33] E. M. Schuman and D. V. Madison, "Nitric oxide and synaptic function," *Annu. Rev. Neurosci.*, vol. 17, pp. 83–153, 1994, doi: 10.1146/annurev.ne.17.030194.001101.

[34] D. S. Bredt and S. H. Snyder, "NITRIC OXIDE: A physiologic messenger molecule," *Annu. Rev. Biochem.*, vol. 63, no. 1, pp. 175–195, Jun. 1994.

[35] O. von Bohlen und Halbach and R. Dermietzel, *Neurotransmitters and Neuromodulators: Handbook of Receptors and Biological Effects*. Weinheim, Germany: Wiley, 2002.

[36] S. R. Y. Cajal, "Significación fisiológica de las expansiones protoplásmiticas y nerviosas de las células de la substancia gris," *Rev. Ciencias Méd.*, vol. 17, pp. 673–679 and 715–723, 1891.

[37] S. R. Vincent, *Nitric Oxide in the Nervous System*. New York, NY, USA: Academic, 1995.

[38] E. Talavera Cuevas, M. Condes-Lara, and G. Martínez-Lorenzana, "Aspectos sobre las funciones del óxido nítrico como mensajero celular en el sistema nervioso central," *Salud Mental*, vol. 26, no. 2, pp. 42–50, 2003.

[39] T. Rajpurohit and W. Haddad, "Stochastic thermodynamics: A dynamical systems approach," *Entropy*, vol. 19, no. 12, p. 693, Dec. 2017.

[40] W. Haddad, "A unification between dynamical system theory and thermodynamics involving an energy, mass, and entropy state space formalism," *Entropy*, vol. 15, no. 12, pp. 1821–1846, May 2013.

[41] P. A. Chou, "The capacity of the Kanerva associative memory is exponential," in *Proc. Neural Inf. Process. Syst.*, D. Z. Anderson, Ed. New York, NY, USA: American Institute of Physics, 1988, pp. 184–191.

[42] P. A. Chou, "The capacity of the Kanerva associative memory," *IEEE Trans. Inf. Theory*, vol. 35, no. 2, pp. 281–298, Mar. 1989.

[43] L. A. Jaeckel, "An alternative design for a sparse distributed memory," Res. Inst. Adv. Comput. Sci., NASA Ames Res. Center, Tech. Rep. 89.28, 1989, vol. 47.

PABLO FERNÁNDEZ-LÓPEZ was born in Gran Canaria, Canary Islands, Spain. He received the M.S. and Ph.D. degrees in computer science from the Universidad de Las Palmas de Gran Canaria.

Since 1998, he has been the Head of Research and Development Area at DESIC (Software Development Firm), he has worked in the development of various intelligent software systems for the control and planning of passenger transport. He is currently an Assistant Professor in computer sciences and artificial intelligence at the Universidad de las Palmas de Gran Canaria (ULPGC). He has published several scientific papers and the results of his work have been presented at international conferences all over the world. His research interests include to study the dynamic of nitric oxide (NO) as an underlaying mechanism of volume transmission (VT) the capabilities of NO in cellular signaling, information transmission, and learning.

PATRICIO GARCÍA-BÁEZ was born in Tenerife, Canary Islands, Spain. He received the M.S. and Ph.D. degrees in computer science from the Universidad de Las Palmas de Gran Canaria.

He is currently an Assistant Professor at the Department of Computer Systems Engineering, Universidad de La Laguna, Spain. He teaches courses related to artificial intelligence, intelligent systems, and artificial neural networks with the School of Computer Science. His research interests include artificial neural networks, which has led him to publish several articles and contribute to the participation and organization of various conferences and seminars. The focus areas of his works are the design of new neural architectures and application in the field of clinical diagnosis and the processing of biological and environmental signals. His research proposals are based on self-organized learning models that are induced in the adaptive capacities of possible changes occurring in their information environments.

YLERMI CABRERA-LEÓN was born in Las Palmas de Gran Canaria, Canary Islands, Spain, in 1987. He received the degree in computer engineering from the Universidad de Las Palmas de Gran Canaria (ULPGC), Spain, in 2015, where he is currently pursuing the Ph.D. degree in business, internet and communications technologies through the Doctoral Program.

His Ph.D. thesis is related to the early detection of Alzheimer's Disease and Mild Cognitive Impairment by means of neural methods. He has co-supervised an undergraduate research project and has served as a tutor for several undergraduate students. His research interests include spam filtering, intelligent computing application in clinical decision making systems for dementia, and Alzheimer's disease.

JUAN L. NAVARRO-MESA (Member, IEEE) was born in la Gomera, Canary Islands, Spain, in 1966. He received the M.S. and Ph.D. degrees in telecommunications engineering from the Polytechnic University of Catalonia, Spain.

He is currently an Associate Professor at the Department of Signal and Communications and the Institute for Technological Development and Innovation in Communications, Universidad de Las Palmas de Gran Canaria. He has extensive research experience in artificial intelligence, data mining, machine learning (and deep learning), and data science. He is involved in the development of clinical decision support systems and weather monitoring and forecasting systems. He has led and participated in international project, patents, publication in journals, national and international congresses, and supervision of Ph.D. theses.

CARMEN PAZ SUÁREZ-ARAUJO received the M.S. degree in physics and the Ph.D. degree in computer science from ULPGC.

She is currently a Professor in computer sciences and artificial intelligence at the Universidad de las Palmas de Gran Canaria (ULPGC), where she is also the Head of the Computational Neuroscience Research Division, Institute of Cybernetics Science and Technology. She is also the Head of the Intelligent Computing with the Perception and Big Data Research Group, ULPGC, where she has been the Director of Ph.D. Programs of Neural Computing in Natural and Artificial Systems. Her research work, which has been awarded by Spanish and international institutions, is focused in natural and artificial neural networks; design of new neural architectures; application of neural computing in clinical, biomedical, environmental domains; computational neuroscience and cognitive computation; and intelligent computing for translational and personalized medicine (non-communicable diseases associated with ageing).

Dr. Suárez-Araujo serves as a Reviewer of Springer, Elsevier, IEEE, *Oxford Academic*, World Scientific, Wiley, and Plos-One. She is an evaluator of international and national evaluation agencies.